Simultaneous Recording of Electrical and Panoramic Optical Mapping From Ex-vivo Isolated Rabbit Hearts: From Sinus Rhythm to Induced Arrhythmia

J Siles [1], I Uzelac[2], V Silva[1], I Sandoval[1], G Weber[1], J Salinet[1]

[1] HEartLab, Federal University of ABC, São Bernardo do Campo, Brazil
[2] Georgia Institute of Technology, Georgia, USA

Abstract

Cardiovascular diseases (CVDs) are the leading causes of death globally, responsible for approximately 52.86% of deaths in Brazil. CVDs modify the characteristics of excitation and electrical propagation of the heart, making electrophysiological tests essential for diagnosis. Current commercial equipment used for clinical evaluation of the substrate can distort the electrograms, resulting in an erroneous diagnosis. Ex-vivo animal models have been developed to characterize the cardiac substrate to improve commercial medical equipment. For this study, New Zealand isolated rabbit hearts were Langendorff perfused and the epicardial electrical activity was acquired simultaneously with a panoramic optical mapping (using the Di-4-ANBDQPQ Voltage-sensitive dye), and a contact electrical mapping setup under sinus rhythm, electrical pacing and during arrhythmia. Finally, the 3D reconstruction subsystem obtained images around the heart and generated a 3D heart. After 18 months of development, seven experiments were performed, signals were synchronized, and metrics such as local activation time were analyzed. This study is significant for improving current knowledge of complex arrhythmia mapping and, more importantly, correct substrate characterization to improve current rates of successful treatment.

1. Introduction

Cardiovascular diseases (CVDs) are the leading causes of death globally, responsible for approximately 52.86% of deaths in Brazil [1]. CVDs modify the characteristics of excitation and electrical propagation of the heart, leading to modifications in the conduction system [2].

Electrophysiological tests are essential for the mechanism's identification for the specific treatment [3]. However, for complex arrhythmias, such as atrial and ventricular fibrillation, the current commercial systems used for clinical evaluation of the substrate can distort the electrograms, resulting in an erroneous diagnosis and reducing the patient's quality of life [3].

Factors such as far-field effects, electrical mapping system type, duration of the recorded signals, and the number of electrodes can influence the identification of mechanisms [4]. Current commercial systems do not provide information about the repolarization characteristics of electrically active cells, and they are sensitive to inter-electrode spacing and wavefront orientation [5].

Optical mapping is an advance considered a gold standard, its use has allowed for better identification of arrhythmia initiation and maintenance mechanisms. In these systems, voltage-sensitive dyes alter their emission spectrum proportionally to voltage changes of transmembrane myocardial cells, allowing a high spatiotemporal resolution mapping of the heart's electrical activity [6]. The fluorescent signal is more proportional to the potential of transmembrane than the electrogram by an electrode; it is also less dependent on the direction of wavefront propagation compared to bipolar electrodes or a large number of unipolar electrodes, and optical signals are more immune to contamination of far-field electrical activity [5]. Further, with more cameras is possible to obtain a panoramic vision of the all heart [7].

This study presents the initial results of a novel experimental model that simultaneously employs electrical and optical panoramic mapping to record and process data in sinus rhythm, pacing, and during arrhythmia. The study outlines the setup configuration, data acquisition process, and data pre-and post-processing procedures. Although this approach is still under development, custom signals, and personalized imaging would improve the current limitations of commercial systems.

2. Methods

2.1. Experimental setup

The experimental setup could be divided into panoramic optical mapping, electrical mapping, and the 3D generation subsystems.

2.1.1. Panoramic optical mapping

Figure 1 presents the excitation system (green lines) consisting of three high-power deep-red LEDs (650 nm, Luminus Devices Inc., USA) placed on a heatsink. Each LED light was collimated (Aspheric Condenser Lens, Thorlabs) and band-pass filtered (650/40 nm Thorlabs) before reaching the heart epicardia. The LED intensity was controlled with a custom in-house LabVIEW GUI (version 21, National Instruments), controlling the DC power supply. The emitted fluorescence was passed through a long pass filter (715 nm, Semrock, USA) on each of the three cameras (Emergent technologies) with a C-mount lens (yellow lines) and each camera was separated 120° between them. The high-speed digital video recording software StreamPix 9 was used to acquire images at 500 frames/s for the three cameras simultaneously at a resolution of 1000x1264 pixels for 10 seconds (5000 images). Cameras were configured to work in a trigger source mode activated for hardware, by GPI5 input, and ending internally.

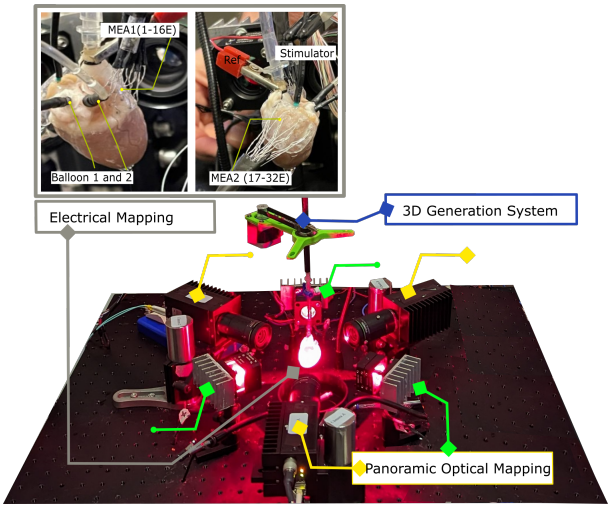

Figure 1. Experimental setup, presenting the panoramic optical mapping (green and yellow lines), the electrical mapping (MEAs, balloons, and pacing electrode), and the 3D generation subsystems.

2.1.2. Electrical mapping

The epicardium electrical activity was acquired using two handmade multi-electrode arrays (MEAs) with 16 silver electrodes positioned in a 4x4 arrangement on a polyethylene terephthalate (PET) surface (Fig. 1 gray) one of 1.4 x 1.5 cm (MEA1) and 2.4 x 1.8 cm (MEA2). Both MEAs were connected to a 64-channel recording headstage (RHD 64-Channel Recording Headstages, C3315, Intan Technologies) through 36-pin wire adapters (C3420, Intan Technologies) to the acquisition Board Open Ephys (Open Ephys acquisition board, Open-source Electrophysiology), allowing acquisition of the epicardial electrograms at 4 kHz.
Arrhythmia was induced by electrical pacing with a bipolar electrode (internal distance between electrodes 2 mm) mounted on a support, allowing contact with the heart. The interval between stimuli could be programmed for pacing or S1-S2 protocol. To prevent chamber collapse, latex balloons were developed allowing the atrium to remain expanded. They were inserted through the pulmonary veins (LA) and the superior vena cava (Fig. 1 gray).

2.1.3. 3D generation

The subsystem presents a customized three-pointed adapter printed with a 3D printer, an Arduino Uno, a bipolar stepper motor driver (DRV8825, Texas Instrument), and a stepper motor (JK35HS34-1004) connected to a belt in the central part of the star-shaped device (Fig. 1 Blue). The toolbox driver software Vision Acquisition Software IMAQdx (version 21.0, National Instrument) was used to acquire, display, and save the images. Positioned at a fixed distance, one optical camera records the sequence of 2D images in every 5 degrees of rotation until complete a full rotation. The excitation red LEDs produce uniform light on the heart for later performing silhouette segmentation and 3D surface generation.

2.2. Experimental process

The research protocol described below has been approved by the local Committee on Ethics in the Use of Animals (CEUA), protocol no. 3947230519. Seven New Zealand male rabbits (3.80 $\pm$ 0,17 Kg) were anesthetized with Acepromazine (0.7 g/Kg), Ketamine (50 g/kg), Xylazine (7 g/kg), and Heparin (5000 U). The euthanasia was performed by thoracotomy, under deep anesthesia. Briefly, the thoracic cavity was accessed and quickly opened, and the heart was extracted by cutting at the upper end of ascending aorta [7]. After removal, the heart was washed and dipped with cold cardioplegia solution (in mM, 110 NaCL, 16 KCL, 10 $NaHCO_3$, 16 $MgCL_2.6H_2O$, 1.2 $CaCl_2.2H_20$), to induce bradycardia, by decreasing energy consumption [8]. Tyrode solution in mM 130 NaCL, 4 KCL, 24 $NaHCO_3$, 1.2 NaH_2PO_4, 1 $MgCl_2.6H_2O$, 1.8 $CaCl_2.2H_20$, 10 Glucose $C_6H_{12}0_6$ was perfused trow the aorta. The contraction motion was suppressed using uncoupler (-)-Blebbistatin. The potentiometric dye Di-4-ANBDQPQ (JPW-6003) was previously prepared, and 0.25 mg per heart was used. Two balloons were located inside the atria, and the MEAs were positioned, one over the right atria (MEA1) and another over the left atria (MEA2). The stimulation catheter was located in the left atria (Fig. 1

gray), and the cameras were calibrated to capture the entire heart located in the middle of the setup. The first recording was taken during sinus rhythm with simultaneous optical and electrical recordings controlled by the generator. Later, a pacing baseline of 150, 250, and 350 ms was established. Finally, burst pacing was applied to induce arrhythmia.

2.3. Pre-processing

For electrical signals, 60 Hz was filtered using a 6th-order harmonic filter with a notch filter designed using the "filtfilt" MatLab function. Afterward, a high-pass Butterworth filter with a cutoff of 1.2 Hz and a low-pass filter of 250 Hz were applied. For optical potentials due to the size of the original data and to improve the signal-to-noise ratio, an 8x8 binning was applied, reducing the 1000x1264 pixel array to 125x158 pixels. First, the baseline was restored using a 4th-order Butterworth high-pass filter with a cutoff frequency of 0.5 Hz. Subsequently, the signal was inverted and spatially filtered using a spatio-temporal Gaussian smoothing filter of 3x3 spatial filter kernel size and 1x5 temporal filter kernel size. Finally, electrical signals were normalized between 1 and 0.

2.3.1. Post-procesing

- **Electrical and optical signals:** For local activation time (LAT) detection in electrical signals, the maximum negative slope of the depolarization complex was used [9] for sinus rhythm, pacing (350, 250, 150 ms), and after the induction of supraventricular arrhythmia [10]. For 2D mapping, the coordinates of the interpolation points were defined as the electrode positions according to the optical camera's images. The function values at the interpolation points were the LAT acquired for the 16 electrodes creating a mesh of interpolated points. Values were interpolated using the griddata function. For optical action potential, LAT detection was calculated using the time of dF/dt_{max} and was expressed in ms [6] to generate LAT maps using the Matlab function imagesc. To compare optical and electrical LATs, the optical sample frequency had to be interpolated to 4 kHz, and the substracts the electrical LAT.
- **3D reconstruction images:** To obtain the 3D surface, silhouette identification was done using image processing and analysis in Java (ImageJ). Then, each region of interest (ROI) was projected over the volume along its respective direction (0°, 120° and 240°, respectively), each voxel outside the ROI was removed. After, the volume contour was obtained by verifying each voxel neighbor, and these were used to get a triangular mesh using the Poisson method [11]. Finally, the mesh was simplified by merging close vertices until reached a number of vertices between 2500 and 3000, and the optical maps projected over.

3. Results

Electrical and optical signals were analyzed simultaneously during sinus rhythm, pacing, and arrhythmia, and local activation times (LATs) are denoted by a black star in Figure 2. Figure 2A shows signals from one electrode located on the right atria and one pixel adjacent to it, with an average LAT difference of -3.1 ms $\pm$ 10.9 ms (11 beats). Figure 2B shows both signals during pacing at 350 ms, with an average LAT difference of -6.7 ms $\pm$ 1.4 ms (14 beats). Finally, Figure 2C presents the signals during supraventricular tachycardia, with an average time difference between them of -1.9 ms $\pm$ 4.1 ms (18 beats).

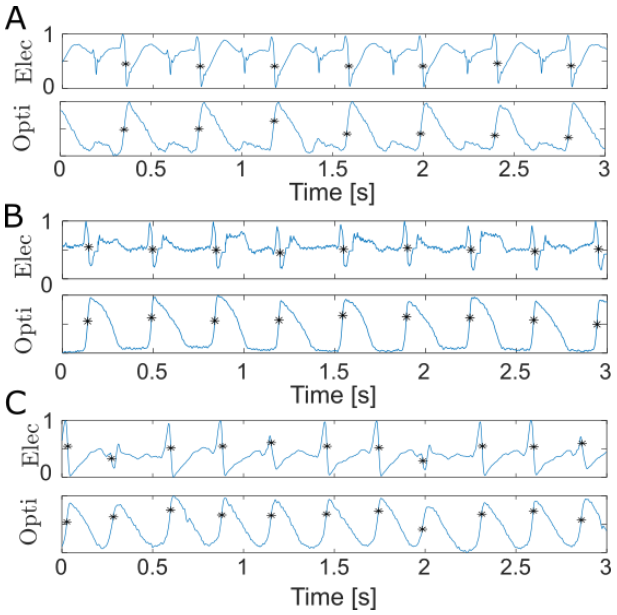

Figure 2. A. Electrical and optical signals obtained for 3 seconds during sinus rhythm (right atria). B. Pacing of 350ms (left atria). C. Supraventricular tachycardia (left atria).

Figure 3A presents an image of one view of the rabbit heart with the MEA1 over the right atria; in the middle, the LAT time map generated using the fluorescence acquired with camera three, and at right, the LAT map generated with the electrical LATs. Figure 3B shows the activation maps generated for the fluorescence images obtained from the three cameras of the setup. At right, the resulting 3D surface heart with the maps projected over.

4. Discussion

This study compared data obtained using panoramic optical and electrical mapping systems over the epicardium [4]. Initially, signals and maps were compared in the area where electrical signals were recorded. Figure 3B showed

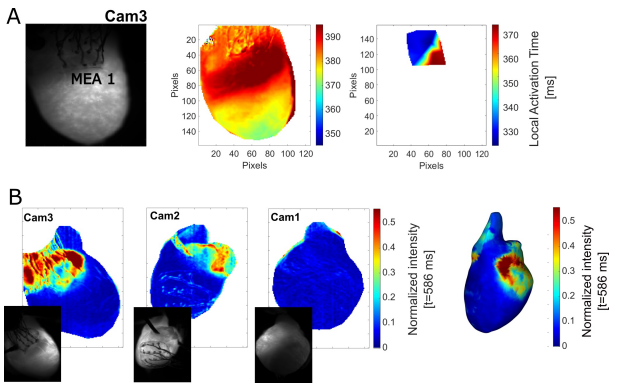

Figure 3. A. Image acquired from camera 3 of the heart and the MEA (left), the optical LAT maps (middle), and the electrical LAT map during sinus rhythm B. Normalized intensity at time=586 ms. for the three optical cameras views and the corresponding 3D surface with the optical maps projected

an unexpected wavefront propagation with no apparent atrial activity. However, electrical activity confirmed an activity that could be atrial. For electrical mapping, a fair-field was something that was expected. However, for optical mapping that uses infrared light, factors such as the atrial thickness, balloon material, and MEA shape may affect the optical action potentials.

5. Conclusion

We recorded simultaneous electrical and panoramic optical mapping recordings from *in-vivo* isolated rabbit hearts under sinus rhythm, pacing, and induced arrhythmia conditions. Initial analysis of these recordings was presented. The setup is under development to identify and map AF mechanisms to customize signal and image processing techniques used by commercial electrical mapping systems using simultaneous analysis of the entire heart at high resolution.

Acknowledgments

J. Siles is supported by grant #2020/03601-9, São Paulo Research Foundation (FAPESP). I. Uzelac and J. Salinet are supported by grant #2018/25606-2, São Paulo Research Foundation (FAPESP). I. Sandoval is supported by the Coordination for the Improvement of Higher Education Personnel (CAPES).

References

[1] Bastos L, Oliveira GMM, Villela PB, Feliciano SCC, Bichara JLP. Social determinants and mortality from cardiovascular disease in brazil. European Heart Journal 10 2021;42.

[2] Garry DJ, Yannopoulos D, Alexy T. Revolutionizing cardiovascular medicine: targeted therapies for the cardiac conduction system. Journal of Clinical Investigation 2022; 132(20):e164192.

[3] Salinet J, Molero R, Schlindwein FS, Karel J, Rodrigo M, Rojo-Álvarez JL, Berenfeld O, Climent AM, Zenger B, Vanheusden F, et al. Electrocardiographic imaging for atrial fibrillation: a perspective from computer models and animal experiments to clinical value. Frontiers in Physiology 2021; 12:653013.

[4] Berenfeld O, Ennis S, Hwang E, Hooven B, Grzeda K, Mironov S, Yamazaki M, Kalifa J, Jalife J. Time-and frequency-domain analyses of atrial fibrillation activation rate: the optical mapping reference. Heart Rhythm 2011; 8(11):1758–1765.

[5] Cantwell CD, Roney CH, Ng FS, Siggers JH, Sherwin SJ, Peters NS. Techniques for automated local activation time annotation and conduction velocity estimation in cardiac mapping. Computers in Biology and Medicine 2015; 65:229–242.

[6] Laughner JI, Ng FS, Sulkin MS, Arthur RM, Efimov IR. Processing and analysis of cardiac optical mapping data obtained with potentiometric dyes. American Journal of Physiology Heart and Circulatory Physiology 2012; 303(7):H753–H765.

[7] Lou Q, Li W, Efimov IR. Multiparametric optical mapping of the langendorff-perfused rabbit heart. JoVE Journal of Visualized Experiments 2011;(55):e3160.

[8] Dhein S. The langendorff heart. In Practical Methods in Cardiovascular research. Springer, 2005; 155–172.

[9] Amino M, Yoshioka K, Tanabe T, Tanaka E, Mori H, Furusawa Y, Zareba W, Yamazaki M, Nakagawa H, Honjo H, Yasui K, Kamiya K, Kodama I. Heavy ion radiation up-regulates Cx43 and ameliorates arrhythmogenic substrates in hearts after myocardial infarction. Cardiovascular Research 12 2006;72(3):412–421.

[10] Guérard N, Jordaan P, Dumotier B. Analysis of unipolar electrograms in rabbit heart demonstrated the key role of ventricular apicobasal dispersion in arrhythmogenicity. Cardiovascular Toxicology 2014;14:316–328.

[11] Kazhdan M, Bolitho M, Hoppe H. Poisson surface reconstruction. In Proceedings of the Fourth Eurographics Symposium on Geometry Processing, volume 7. 2006; 0.

Address for correspondence:

Jimena Gabriela Siles Paredes
Biomedical Engineering - CECS
Federal University of ABC - UFABC
Street: Av. Anchieta, São Bernardo do Campo - SP, Brazil
E-mail: jimena.gabriela@ufabc.edu.br